of the arsolane ring species, this influence of methyl substitution on ring stability is consistent with that observed for arsenium ion stability.

All of the arsenic-containing ions in these aminoarsolanes can be assigned structures in which arsenic is monovalent/divalent or divalent/trivalent. No major peaks in the spectra can be assigned structures containing the As=O bond or trivalent/tetravalent arsenic. Such results are in agreement with those of Frøyen and Møller[24,43] for 2-substituted 1,3,2-dioxarsenanes and esters of arsenious acid and may be related to the thermodynamic stability of the As=O bond.[43]

Frøyen and Møller[24] observed that the main fragmentation route for the $[M - R]^+$ ion in the substituted 1,3,2-dioxarsenanes was caused by the loss of CH_2O and that, in some cases, the molecular ion directly eliminated aldehyde. Such elimination is not observed for $OCH_2CH_2OAsN(C_2H_5)_2$ and $OCH_2CH_2OAsN(n\text{-}C_3H_7)_2$ but appears to be an important process in the fragmentation of the methyl and ethyl derivatives of the 2-(dialkylamino)-4,4,5,5-tetramethyl-1,3,2-dioxarsolanes.

(43) Frøyen, P.; Møller, J. *Org. Mass Spectrom*, **1973**, *7*, 73.

Acknowledgment. The support from the Research Corp. and the University College Committee on Faculty Research Grants at the University of Alabama in Birmingham is acknowledged. The assistance of Dr. R. King at the University of Florida in obtaining the mass spectra is greatly appreciated.

Registry No. OCH_2CH_2OAsCl, 3741-33-1; $OCH_2CH_2OAsN(CH_3)_2$, 27262-85-7; $OCH_2CH_2OAsN(C_2H_5)_2$, 34713-88-7; $OCH_2CH_2OAsN(n\text{-}C_3H_7)_2$, 74466-67-4; $OC(CH_3)_2C(CH_3)_2OAsCl$, 54128-06-2; $OC(CH_3)_2C(CH_3)_2OAsN(CH_3)_2$, 57938-74-6; $OC(CH_3)_2C(CH_3)_2OAsN(C_2H_5)_2$, 74466-68-5; $OC(CH_3)_2C(CH_3)_2OAsN(n\text{-}C_3H_7)_2$, 74466-69-6; $[OC(CH_3)_2C(CH_3)_2OAs]_2NH$, 74466-70-9; $[OC(CH_3)_2C(CH_3)_2OAs]_2NCH_3$, 74466-71-0; $OC(CH_3)_2C(CH_3)_2OAsNH(n\text{-}C_4H_9)$, 74466-72-1; $OCH_2CH_2OAsOCH_2CH_2OAsOCH_2CH_2O$, 14849-23-1; $As_4[N(n\text{-}C_4H_9)]_6$, 3690-32-2; $(n\text{-}C_3H_7)_2NH$, 142-84-7; $n\text{-}C_4H_9NH_2$, 109-73-9; CH_3NH_2, 74-89-5; NH_3, 7664-41-7.

Supplementary Material Available: A listing of infrared and mass spectral data (4 pages). Ordering information is given on any current masthead page.

Contribution from the School of Chemical Sciences, University of Illinois, Urbana, Illinois 61801, and the Research School of Chemistry, The Australian National University, Canberra, A.C.T., Australia

Metal Complexes of Diiminodiphosphines. Structural and Reactivity Patterns

JOHN C. JEFFERY, THOMAS B. RAUCHFUSS,* and PAUL A. TUCKER

Received June 4, 1980

The coordination chemistries of *N,N'*-bis[*o*-(diphenylphosphino)benzylidene]ethylenediamine (en=P_2) and the corresponding 1,3-diaminopropane derivative (tn=P_2) have been explored for the metals nickel, copper, and silver, and these results provide fundamental information on this novel class of metal complexes. The ligands function as tetradentate chelating agents for these metal ions as inferred from spectroscopic data and proven by the X-ray structure of $[Cu(en{=}P_2)]ClO_4{\cdot}CH_2Cl_2$, the first iminophosphine chelate thus characterized. The crystals are triclinic, of space group $P\bar{1}$, with a = 14.140 (3) Å, b = 24.926 (5) Å, c = 11.430 (3) Å, α = 94.45 (1)°, β = 81.91 (1)°, γ = 97.42 (1)°, and Z = 4. The complex adopts a severely distorted tetrahedral geometry, and this strain is manifested in its reactivity. The four-coordinate complexes $M(en{=}P_2)^z$ (M = Cu or Ag, z = 1+; M = Ni, z = 2+) all react with additional ligands L (M = Ag or Cu, L = *tert*-butyl isocyanide (*t*-BuNC); M = Ni, L = Br^-), affording five-coordinate adducts in the case of Ni(II) and Ag(I). Crystals of the derivative $[Cu(en{=}P_2)(t\text{-}BuNC)]ClO_4$, examined by X-ray methods show the metal to be tetrahedrally coordinated. The first coordination sphere contains only one imine functionality in addition to the isocyanide and the two phosphine moieties. The crystals are orthorhombic, of space group $P222$, with a = 30.232 (9) Å, b = 16.144 (4) Å, c = 8.450 (2) Å, and Z = 4. The complex is a unique example of a nine-membered chelate ring bound to a tetrahedral complex and is formed by the displacement of an internal donor of the chelate. All complexes are dynamic on the NMR time scale (−80 to 35 °C), and mechanisms consistent with the spectroscopic and X-ray data are presented. The electrochemical behavior of the complexes demonstrate the interconvertability of the $[M(en{=}P_2)]^z$ unit containing the metal ion in the d^8, d^9, and d^{10} configurations for M = Ni or Cu. The impact of the additional methylene group in the tn=P_2 complexes vs. the en=P_2 analogues is assessed chemically and electrochemically.

Introduction

A characteristic of the coordination chemistry of chelating bis(tertiary phosphines and arsines) is their distinctive ability to stabilize metal ions in a variety of uncommon oxidation states and geometries.[1] The adaptive nature of these ligands is a desirable attribute, from both theoretical[2] and applied (e.g., catalysis[3]) perspectives. Imino ligands, particularly the 1,2-diimines,[4] are also known to stabilize metal ions in a variety of low and high oxidation states, and their metal complexes are powerful catalysts in both biological (e.g., corrins, porphyrins) and industrial roles (e.g., phthalocyanins). Being a fusion of these ligand types, the iminophosphines hold promise to provide a new and readily available source of ligands which retain many of the aforementioned properties of imines and phosphines. A variety of iminophosphines[5-9] and iminoarsines[10]

* To whom correspondence should be addressed at the University of Illinois.

(1) Warren, L. F.; Bennett, M. A. *Inorg. Chem.* **1976**, *15*, 3126–3140.
(2) Bernstein, P. K.; Gray, H. B. *Inorg. Chem.* **1972**, *11*, 3035–3039.
(3) Fryzuk, B. N.; Bosnich, B. *J. Am. Chem. Soc.* **1978**, *100*, 5491–5494.
(4) For instance see: Staal, L. H.; Oskam, A.; Vrieze, K.; Roosendahl, E.; Schenk, H. *Inorg. Chem.* **1979**, *18*, 1634–1640.
(5) Sacconi, L.; Speroni, G. P.; Morassi, R. *Inorg. Chem.* **1968**, *7*, 1521–1525.
(6) DuBois, T. D. *Inorg. Chem.* **1972**, *11*, 718–722.
(7) Riker-Nappier, J.; Meek, D. W. *J. Chem. Soc., Chem. Commun.* **1974**, 442–443.

0020-1669/80/1319-3306$01.00/0

have been prepared although so far their coordination chemistry has been restricted to the derivatives of divalent metal ions. Prior to the work of one of us[9] these ligands were synthesized from the condensation of organic carbonyls with aminophosphines or aminoarsines. As part of a broader program concerned with exploring the synthetic utility of the carbonyl phosphines, e.g., *o*-(diphenylphosphino)benzaldehyde, we have prepared derivatives in which the formyl group has been converted to an imine; this methodology enjoys distinct advantages over the previously reported route to these imino containing hybrid ligands in both synthetic versatility and convenience.

Herein we report a study of the stereochemical and reactivity patterns of metal complexes of two diiminodiphosphines including the first crystallographic examination of this class of coordination compounds. We also describe a novel substitution pattern for metal complexes of polydentate ligands which was uncovered in the course of these studies. The results reported herein represent the basis for the design and synthesis of more complex and stereoselective ligands applicable to asymmetric catalysis.

Experimental Section

^{1}H nuclear magnetic resonance spectra were recorded variously on a 90-MHz Jeol Minimar, 90-MHz Varian EM390, or 100-MHz HA 100 spectrometer. ^{31}P NMR spectra (Bruker 90 or a Varian XL100 spectrometer) were always ^{1}H decoupled. Microanalyses were obtained at both The Australian National University and the University of Illinois with the in-house services. *o*-(Diphenylphosphino)benzaldehyde was prepared according to Schiemenz and Kaack,[11] by using commercially available *o*-bromobenzaldehyde (Fluka, Aldrich) and diphenylphosphinous chloride (Aldrich). *tert*-Butyl isocyanide was prepared by using a modified literature method[12] by Mr. Horst Neumann at The Australian National University or purchased from Strem Chemicals. All compounds reported in the Experimental Section gave satisfactory microanalyses for CHNP; these data are contained in the supplementary material. (See the paragraph at the end of this paper regarding supplementary material.)

***N,N'*-Bis[*o*-(diphenylphosphino)benzylidene]ethylenediamine, en=P$_2$ (1).** *o*-$Ph_2PC_6H_4CHO$, 29 g (0.1 mol), and 3.3 mL of freshly distilled ethylenediamine (0.05 mol) were refluxed with stirring in 300 mL of absolute ethanol for 90 min. After this time, the cream-colored slurry was cooled to 0 °C for 12 h and filtered; the product was rinsed with EtOH and air-dried. The yield was 25.5 g (85%). While this material was satisfactory for the preparation of complexes, it was necessary to recrystallize a small portion from CH_2Cl_2/EtOH to obtain an analytically pure sample.

Four-Coordinate en=P$_2$ Complexes. $[Cu(MeCN)_4]ClO_4$, 314 mg (0.97 mmol), was dissolved in 25 mL of MeCN. A solution of 610 mg (1.01 mmol) of en=P$_2$ in 10 mL of CH_2Cl_2 was added, and the solution instantly changed from colorless to dark orange. The solution was then diluted with 100 mL of Et_2O. After 2 h, the crystals of $[Cu(en{=}P_2)]ClO_4$ (**2**) were collected and washed with Et_2O. The yield was 700 mg (60%). The silver(I) (**3**) and nickel(II) (**4**) fluoroborates were prepared similarly. The MeCN solution of the nickel complex is brown, while the CH_2Cl_2 solutions of the same compound are yellow, suggesting that the brown coloration is due to $[Ni(MeCN)(en{=}P_2)]^{2+}$.

[Cu(tn=P$_2$)]ClO$_4$ (5). A sample of 960 mg of PCHO (3.33 mmol) and 140 μL of 1,3-diaminopropane (tn) (1.66 mmol) were refluxed in 30 mL of absolute EtOH, yielding after evaporation an oily product which was redissolved in ca. 80 mL of CH_2Cl_2. A solution of 545 mg of $[Cu(MeCN)_4]ClO_4$ (1.66 mmol) in ca. 50 mL of MeCN was added to the CH_2Cl_2 solution, producing a yellow-orange solution which was then diluted with 300 mL of Et_2O and 500 mL of petroleum ether (bp 100 °C). After cooling of the solution for 1 h, the crystalline precipitate was collected and recrystallized from CH_2Cl_2 by the addition of ether, yielding 1.09 g (84%).

[Ni(tn=P$_2$)](BF$_4$)$_2$ (6). A sample of 870 mg of PCHO (3 mmol) and 110 mg of 1,3-diaminopropane (tn) (1.5 mmol) was refluxed in 30 mL of EtOH for 3 h. After cooling of the solution to room temperature, 535 mg of $[Ni(H_2O)_6](BF_4)_2$ (1.5 mmol) was added, and the orange solution was refluxed for 1 h. The cooled solution was filtered, and the solid was extracted with acetone, filtered, and evaporated. This material was recrystallized by dissolution of the solid in methanol/acetone (1:1) and dilution with Et_2O. The yield was 740 mg (53%).

[Cu(en=P$_2$)(*t*-BuNC)]ClO$_4$ (7) and [Ag(en=P$_2$)(*t*-BuNC)]BF$_4$ (8). An excess of *t*-BuNC (~5 drops) was added to a solution of 100 mg of $[Ag(en{=}P_2)]BF_4$ in CH_2Cl_2 (10 mL), resulting in the rapid formation of a pale yellow color. The solution was then slowly diluted with hexane, yielding cream crystals. The yield was 93 mg (84%). The copper complex $[Cu(en{=}P_2)(t\text{-BuNC})]ClO_4$ was prepared similarly.

[NiBr(en=P$_2$)]Br (9). A sample of 604 mg of en=P$_2$ (0.5 mol) in 10 mL of CH_2Cl_2 was added to a stirred solution of $NiBr_2{\cdot}3H_2O$ (0.5 mmol) in 20 mL of EtOH. The brown solution was stirred for 1 h, filtered, rinsed with 10 mL of CH_2Cl_2, and diluted with 175 mL of Et_2O with stirring to give brown crystals. Recrystallization from CH_2Cl_2/Et_2O yielded 675 mg (82%) of red-brown crystalline complex.

Electrochemistry. The instrumentation has been described previously.[13] Measurements on the en=P$_2$ complexes were made by using a Pt working electrode and ~10^{-3} M solutions of the metal complexes in a 0.1 M acetone solution of tetraethylammonium perchlorate. Measurements on the tn=P$_2$ complexes were made by using an Au electrode and working in 0.1 M acetonitrile solution of tetramethylammonium trifluoromethylsulfonate. The reference electrode in all cases was Ag/AgCl (0.1 M LiCl in MeCN).

Collection and Reduction of X-ray Intensity Data. [Cu(en=P$_2$)]ClO$_4$. Crystals of $[Cu(en{=}P_2)][ClO_4]{\cdot}CH_2Cl_2$ were obtained from CH_2Cl_2/hexane and were coated with a thin film of Araldite to inhibit loss of solvent. The crystal used for data collection was a well-developed parallelepiped with {010}, {001}, and {110} faces and maximum

Table I. Crystal and Data Collection[a] Details for $[Cu(en{=}P_2)]ClO_4{\cdot}CH_2Cl_2$ and $[Cu(en{=}P_2)(t\text{-BuNC})]ClO_4$

	$[Cu(en{=}P_2)]ClO_4{\cdot}CH_2Cl_2$	$[Cu(en{=}P_2)(t\text{-BuNC})]ClO_4$
empirical formula	$C_{41}H_{36}Cl_3CuN_2O_4P_2$	$C_{45}H_{43}ClCuN_3O_4P_2$
fw	852.6	850.8
a, Å	14.140 (3)	30.232 (9)
b, Å	24.926 (5)	16.144 (4)
c, Å	11.430 (3)	8.450 (2)
α, deg	94.45 (1)	90
β, deg	81.91 (1)	90
γ, deg	97.42 (1)	90
V_c, Å^3	3947.8	4124.2
ρ_{obsd},[b] g cm^{-3}	1.44 (1)	1.37 (1)
Z	4	4
ρ_{calcd}, g cm^{-3}	1.41	1.37
space group	$P\bar{1}$ (C_i, No. 2)	$P2_12_12_1$ (D_2^4, No. 19)
scan speed, deg min^{-1}	2.0	0.9
scan width,[c] deg	$(2\theta - 0.9)$–$(2\theta + 0.9 + \Delta)$	$(0.8 + 0.34 \tan \phi)$
max 2θ, deg	50	45
data collected	15 041	6246
unique data with $I > 3\sigma(I)$	9076	2848

[a] Intensities were measured with graphite-monochromated Mo Kα radiation ($2\theta_m = 12.16°$, λ(Mo Kα) = 0.710 69 A, tube takeoff angle = 3°) with use of $\theta/2\theta$ scan mode with stationary backgrounds (10 s) at each end of the peak scan. [b] By flotation. [c] Δ is the angular separation of the $K\alpha_1$ and $K\alpha_2$ components of the diffracted beam.

(8) Cabral, J. deO.; Cabral, M. F.; Drew, M. G. B.; Nelson, S. M.; Rogers, A. *Inorg. Chim. Acta* **1977**, *25*, L77–79.
(9) Rauchfuss, T. B. *J. Organomet. Chem.* **1978**, *162*, C19–21.
(10) Chiswell, B.; Lee, K. W. *Inorg. Chim. Acta* **1973**, *7*, 49–59, 509–516, 517–523; **1972**, *6*, 583–590. Lee, K. W. Ph.D. Thesis, University of Queensland, 1971.
(11) Schiemenz, G. P.; Kaack, H. *Liebigs. Ann. Chem.* **1973**, 1480–1493.
(12) Gokel, G. W.; Widera, R. P.; Weber, W. P. *Org. Synth.* **1976**, *55*, 96–99.
(13) Hendrickson, A. R.; Martin, R. L.; Rhoda, N. M. *Inorg. Chem.* **1975**, *14*, 2980–2985.

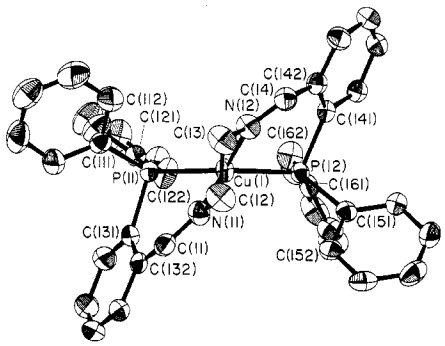

Figure 1. ORTEP drawing and numbering scheme for cation **1** of $[Cu(en{=}P_2)]^+$ with thermal ellipsoids drawn at the 50% probability level.

dimensions of ca. 0.3 × 0.3 × 0.2 mm. Crystals are triclinic, of space group $P\bar{1}$.

Reflection data were collected on a Picker FACS-I automatic four-circle diffractometer, by using Mo Kα radiation. Unit cell dimensions together with their estimated standard errors and the crystal orientation matrix were obtained from the least-squares analysis of the setting angles of 12 carefully centered high-angle reflections.[14] Crystal data and details of the experimental conditions are in Table I.

The intensities of three standard reflections were monitored periodically to check crystal and electronic stability. No significant intensity variations were observed throughout the period of data collection. Reflection intensities were reduced to values of $|F_o|$ and were assigned individual estimated standard deviations ($\sigma(F_o)$).[15] A value of 0.04 was used for the instrumental uncertainty factor (p).[16] Reflection data were sorted, equivalent reflections were averaged, and reflections with $I \geq 3\sigma(I)$ were considered observed. No absorption or extinction corrections were applied to the data. The statistical R factor (R_s)[15] for the terminal data set was 0.028 (9076 reflections).

The structure was solved by using MULTAN[17] in conjuction with conventional Patterson techniques and was refined satisfactorily by using block-diagonal least-squares methods in space group $P\bar{1}$, with two independent pseudocentrosymmetrically related formula units per asymmetric unit ($Z = 4$). MULTAN initially gave a false solution with the two Cu cations incorrectly positioned in the asymmetric unit. Further analysis, based on the initial (false) solution, fortuitously gave a good set of structural parameters for one cation, but it became apparent that these results could not be reconciled in detail with the Patterson synthesis. MULTAN readily gave the correct solution when the derived structural parameters for the one cation were used to calculate accurate group scattering factors for both cations, which once more emphasizes the known usefulness of this approach in direct methods procedures.[17,18]

Atomic and anomalous scattering factors were taken from ref 19. Fixed phenyl hydrogen atom contributions were included in the scattering model (C–H = 0.95 Å, $B_H = B_C$). The final R value was 0.053 (R_w = 0.068). In the last cycle of least-squares refinement, no parameter shifted by more than 0.1 of its estimated standard deviation, and an analysis of the weighting scheme revealed no systematic dependence of $w\Delta^2$ on $|F_o|$ or sin ϕ. The highest radical peaks in the final difference maps were ca. 1.0 e/Å^3. Final atomic coordinates are listed in Table II. Listings of anisotropic thermal parameters and of $10|F_o|$ and $10|F_c|$ have been deposited. The atom numbering in the cation is illustrated in Figure 1.

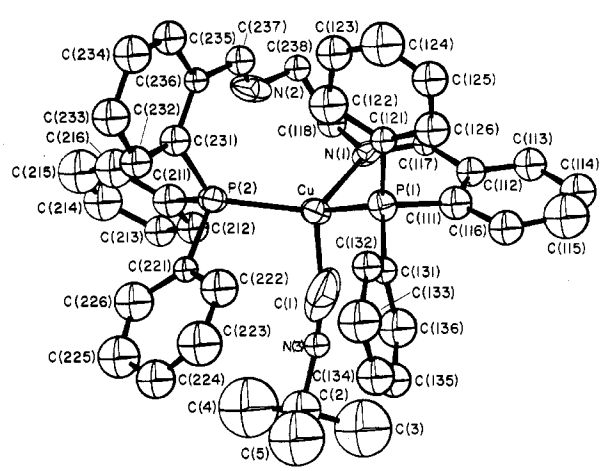

Figure 2. ORTEP drawing and numbering scheme for $[Cu(en{=}P_2)(t\text{-BuNC})]^+$ with thermal ellipsoids drawn at the 50% probability level.

Scheme I

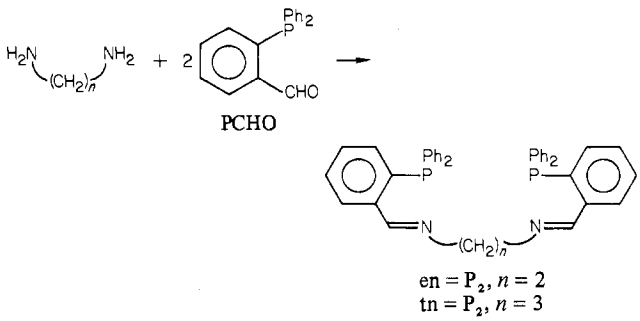

[Cu(en=P$_2$)(*t*-BuNC)]ClO$_4$. Crystals, commonly six-sided needles along (001), were obtained by recrystallization from dichloromethane/hexane solutions. The crystal used for data collection had approximate dimensions 0.01 × 0.05 × 0.01 cm. Crystals are orthorhombic of space group $P222$. Intensities were measured on a Philips PW1100 automatic four-circle diffractometer.[14] Unit cell dimensions and standard errors were measured on a Picker FACS-I diffractometer as described above. Mo Kα radiation was employed for both data collection and cell measurement. Crystal data and experimental conditions are listed in Table I.

Reflection data were measured in the quadrants hkl and $\bar{h}kl$. As before, intensities of the three standard reflections which were monitored periodically remained unchanged (to within experimental error) throughout the experiment. Reflection intensities were reduced to $|F_o|$ and assigned standard deviations, $\sigma(F_o)$, as described in ref 20. Reflection data were sorted, and reflections with $I < 3\sigma(I)$ were rejected as unobserved. No absorption [μ(Mo Kα) = 7.2 cm^{-1}] or extinction corrections were applied. The statistical R factor, R_s,[15] was 0.096 for 2848 reflections.

The structure was solved by conventional Patterson and Fourier techniques and was refined by full-matrix least-squares methods. Atomic scattering factors and the anomalous dispersion corrections for Cu, P, and Cl were taken from ref 19. In view of the high statistical R factor, R_s, no attempt was made to include hydrogen atom contributions or to refine anisotropic thermal parameters for the carbon atoms. The final R was 0.110 (R_w = 0.103). The poor intensity statistics do not allow the determination of the absolute configuration

(14) The programs contained in the Picker Corp. FACS-I Disk Operating System (1972) were used for all phases of the Picker diffractometer control and data collection. All phases of the Philips diffractometer control were by the PW1100/15 control program 11CN20 (1976).

(15) Formulas used in the data reduction programs: Lp (Lorentz–polarization factor) = $(\cos^2 2\theta + \cos^2 2\theta_m)/[(\sin 2\theta)(1 + \cos^2 2\theta_m)]$, where θ and θ_m (−6.08°) are the reflection and monochromator Bragg angles, respectively; I (net peak intensity) = $[CT - (t_p/t_b)(B_1 + B_2)]$, where CT is the total peak count in t_p s, and B_1 and B_2 are the individual background counts in $[(t_p/t_b)^2(B_1 + B_2)]^{1/2}$; $\sigma(F_o)$ (the reflection esd) = $\{[\sigma(I)/Lp]^2 + (p|F_o|)^2\}^{1/2}/2|F_o|$; $\sigma_s(F_o)$ (the reflection esd from counting statistics alone) = $[\sigma(I)/2(Lp)(|F_o|)]$; R_s (the statistical R factor) = $\sum\sigma_s(F_o)/\sum|F_o|$; background rejection ratio = $|B_1 - B_2|/(B_1 + B_2)^{1/2}$.

(16) Busing, W. R.; Levy, H. A.; *J. Chem. Phys.* **1957**, *26*, 563–571. Corfield, P. W. R.; Doedens, R. J.; Ibers, J. A. *Inorg. Chem.* **1967**, *6*, 197–204.

(17) Declerq, J. P.; Germain, G.; Main, P.; Woolfson, M. M. *Acta Crystallogr. Sect. A* **1973**, *A29*, 231.

(18) Main, P. "Crystallographic Computing Techniques"; Munksgaard: Copenhagen, 1976; p 7.

(19) "International Tables for X-ray Crystallography"; Kynoch Press: Birmingham, 1974; Vol. IV.

(20) As for ref 15 except that $\sigma(I)$ and $\sigma(F_o)$ are defined as in the CRSTAN program package: H. Burzlaff, R. Böhme, and M. Gomm, Institut für Angewandte Physik, Universität Erlangen, 1977.

Table II. Atomic Coordinates for $[Cu(en{=}P_2)]ClO_4 \cdot CH_2Cl_2$

ATOM	X/A	Y/B	Z/C
CU(1)	0.42285(4)	0.16495(3)	0.64073(5)
P(11)	0.48306(10)	0.10281(5)	0.72879(11)
P(12)	0.46873(9)	0.21524(5)	0.47214(11)
C(111)	0.3904(4)	0.0601(2)	0.8284(4)
C(112)	0.3091(5)	0.0409(3)	0.7956(6)
C(113)	0.2435(5)	0.0070(3)	0.8669(7)
C(114)	0.2655(5)	-0.0078(3)	0.9691(6)
C(115)	0.3526(5)	0.0110(3)	1.0029(6)
C(116)	0.4188(4)	0.0450(2)	0.9346(5)
C(121)	0.5649(4)	0.0568(2)	0.6519(4)
C(122)	0.6392(4)	0.0777(2)	0.5709(5)
C(123)	0.7048(5)	0.0454(3)	0.5128(6)
C(124)	0.6955(5)	-0.0081(3)	0.5338(6)
C(125)	0.6236(5)	-0.0290(2)	0.6133(6)
C(126)	0.5568(5)	0.0029(2)	0.6713(5)
C(131)	0.5542(4)	0.1425(2)	0.8351(4)
C(132)	0.5175(4)	0.1860(2)	0.9067(4)
C(133)	0.5697(5)	0.2111(2)	0.9949(5)
C(134)	0.6555(5)	0.1956(3)	1.0110(5)
C(135)	0.6942(5)	0.1552(3)	0.9403(6)
C(136)	0.6425(4)	0.1287(2)	0.8537(5)
C(11)	0.4249(4)	0.2059(2)	0.9062(4)
N(11)	0.3857(3)	0.2035(2)	0.8060(3)
C(12)	0.2923(4)	0.2235(3)	0.8129(5)
C(13)	0.2248(4)	0.1789(3)	0.7486(5)
N(12)	0.2782(3)	0.1682(2)	0.6297(4)
C(14)	0.2361(4)	0.1726(2)	0.5408(5)
C(141)	0.3792(3)	0.1774(2)	0.3733(4)
C(142)	0.2807(4)	0.1651(2)	0.4152(4)
C(143)	0.2169(4)	0.1461(2)	0.3356(5)
C(144)	0.2472(4)	0.1368(2)	0.2171(5)
C(145)	0.3416(4)	0.1475(2)	0.1764(5)
C(146)	0.4078(4)	0.1685(2)	0.2518(4)
C(151)	0.4629(3)	0.2784(2)	0.4734(4)
C(152)	0.4660(4)	0.3086(2)	0.5779(4)
C(153)	0.4654(4)	0.3638(2)	0.5847(5)
C(154)	0.4619(4)	0.3894(2)	0.4822(6)
C(155)	0.4586(5)	0.3598(2)	0.3758(5)
C(156)	0.4594(4)	0.3039(2)	0.3709(5)
C(161)	0.5845(3)	0.1974(2)	0.3864(4)
C(162)	0.6060(4)	0.1469(2)	0.3397(5)
C(163)	0.6998(4)	0.1409(3)	0.2801(5)
C(164)	0.7689(4)	0.1833(3)	0.2714(5)
C(165)	0.7491(4)	0.2330(3)	0.3188(5)
C(166)	0.6583(4)	0.2402(2)	0.3760(5)
CU(2)	0.01672(4)	0.33638(2)	0.39104(5)
P(21)	-0.03530(9)	0.40170(5)	0.30451(11)
P(22)	-0.03972(9)	0.30232(5)	0.56471(11)
C(211)	0.0513(4)	0.4472(2)	0.2143(4)
C(212)	0.1467(4)	0.4378(2)	0.1985(5)
C(213)	0.2157(4)	0.4684(2)	0.1238(6)
C(214)	0.1904(5)	0.5098(3)	0.0687(5)
C(215)	0.0955(4)	0.5209(2)	0.0856(5)
C(216)	0.0266(4)	0.4890(2)	0.1569(5)
C(221)	-0.1195(3)	0.4446(2)	0.3878(4)
C(222)	-0.2088(4)	0.4221(2)	0.4363(5)
C(223)	-0.2731(4)	0.4534(3)	0.5038(6)
C(224)	-0.2447(4)	0.5079(3)	0.5273(6)
C(225)	-0.1571(5)	0.5309(2)	0.4840(5)
C(226)	-0.0921(4)	0.4997(2)	0.4137(5)
C(231)	-0.1044(4)	0.3653(2)	0.1892(4)
C(232)	-0.0721(4)	0.3194(2)	0.1232(4)
C(233)	-0.1224(4)	0.2966(2)	0.0315(4)
C(234)	-0.2037(5)	0.3157(2)	0.0078(5)
C(235)	-0.2365(4)	0.3591(2)	0.0724(5)
C(236)	-0.1846(4)	0.3846(2)	0.1618(5)
C(21)	0.0121(4)	0.2934(2)	0.1365(4)
N(21)	0.0481(3)	0.2933(2)	0.2333(3)
C(22)	0.1336(4)	0.2642(2)	0.2314(5)
C(23)	0.2077(4)	0.3015(2)	0.2992(5)
N(22)	0.1556(3)	0.3212(2)	0.4135(3)
C(24)	0.1917(3)	0.3165(2)	0.5072(4)
C(241)	0.0476(3)	0.3308(2)	0.6654(4)
C(242)	0.1477(3)	0.3331(2)	0.6271(4)
C(243)	0.2112(4)	0.3507(2)	0.7075(5)
C(244)	0.1798(4)	0.3691(2)	0.8220(5)
C(245)	0.0849(4)	0.3685(3)	0.8582(5)
C(246)	0.0192(4)	0.3489(2)	0.7807(4)
C(251)	-0.0382(3)	0.2294(2)	0.5678(4)
C(252)	-0.0448(4)	0.1981(2)	0.4643(5)
C(253)	-0.0852(4)	0.1426(2)	0.4609(5)
C(254)	-0.1160(5)	0.1177(2)	0.5651(6)
C(255)	-0.1088(5)	0.1486(2)	0.6690(5)
C(256)	-0.0745(4)	0.2039(2)	0.6718(5)
C(261)	-0.1580(3)	0.3134(2)	0.6452(4)
C(262)	-0.1772(4)	0.3654(2)	0.6793(5)
C(263)	-0.2687(4)	0.3740(3)	0.7367(5)
C(264)	-0.3386(4)	0.3315(3)	0.7544(5)
C(265)	-0.3205(4)	0.2801(3)	0.7185(5)
C(266)	-0.2298(4)	0.2705(2)	0.6644(5)
CL(1)	0.00665(11)	0.13615(6)	0.03024(13)
O(11)	0.0018(4)	0.1462(3)	0.1522(4)
O(12)	0.0471(11)	0.1769(3)	-0.0225(7)
O(13)	0.0591(9)	0.0978(4)	-0.0124(7)
O(14)	-0.0725(6)	0.1220(6)	-0.0006(8)
CL(2)	0.42101(12)	0.35227(7)	0.01396(14)
O(21)	0.3945(7)	0.3989(3)	0.0591(8)
O(22)	0.5134(6)	0.3532(5)	0.0354(7)
O(23)	0.3677(8)	0.3138(3)	0.0743(6)
O(24)	0.4206(9)	0.3393(3)	-0.1077(4)
CL(11)	0.5498(2)	0.4865(1)	0.7716(3)
CL(12)	0.3566(2)	0.5013(1)	0.7523(2)
CL(21)	1.0704(2)	0.0085(1)	0.6650(3)
CL(22)	0.8664(2)	-0.0025(1)	0.7322(3)
C(1)	0.4397(5)	0.4995(4)	0.8485(7)
C(2)	0.9775(6)	-0.0015(4)	0.7892(7)

for the cation. In the last cycle of refinement no parameter shift exceeded 0.2σ. The function minimized, $\sum w(|F_o| - |F_c|)^2$, showed no appreciable dependence on $|F_o|$ or $(\sin\theta)/\lambda$. The highest residual peaks (or troughs) in the final difference maps were ca. 2.0 $Å^{-3}$. Final atomic parameters are listed in Table III, and the atom numbering in the cation is illustrated in Figure 2. Tables of $10|F_o|$ and $10|F_c|$ (electrons) are contained in the supplementary material.

Computer Programs. All calculations were carried out on the Univac 1108 computer of The Australian National University Computer Center, by using previously described programs.[21]

(21) Ferguson, J.; Mau, A. W.-H.; Whimp, P. O. *J. Am. Chem. Soc.* **1979**, *101*, 2363–2369.

Results and Discussion

Ligands. The phosphine aldehyde, PCHO, many of its isomers, and the corresponding acetophenone derivatives were first prepared and characterized by Kaack and Schiemenz.[11] These compounds are potentially valuable ligand percursors via elaboration of the carbonyl group by condensation and/or reductions. The tetradentate ligand *N,N'*-bis[*o*-(diphenylphosphino)benzylidene]ethylenediamine, abbreviated en=P_2 (**1**), is easily prepared by the condensation of 2 equiv of *o*-(diphenylphosphino)benzaldehyde with ethylenediamine in boiling ethanol (Scheme I). This chelating agent is soluble in common organic solvents and is conveniently crystallized

Table III. Atomic Coordinates and Temperature Factors for $[Cu(en{=}P_2)(t\text{-BuNC})]ClO_4$

ATOM	X/A	Y/B	Z/C	BETA11	BETA22	BETA33	$BETA_{12}$	$BETA_{13}$	BETA23
CU	0.1414(1)	0.2472(1)	0.1480(3)	0.0009(1)	0.0025(1)	0.0128(3)	-0.0002(1)	0.0003(1)	0.0000(3)
P(1)	0.2027(1)	0.2603(3)	0.2967(5)	0.0009(1)	0.0035(3)	0.0099(8)	0.0000(1)	0.0000(2)	0.0004(5)
P(2)	0.0714(1)	0.2738(3)	0.2393(6)	0.0007(1)	0.0026(2)	0.0158(10)	-0.0001(1)	-0.0007(2)	0.0009(4)
N(1)	0.1684(5)	0.3153(8)	-0.0322(17)	0.0012(2)	0.0027(7)	0.0107(28)	0.0007(3)	0.0015(7)	0.0024(13)
N(2)	0.0921(5)	0.4159(9)	0.0590(22)	0.0013(3)	0.0029(8)	0.0243(40)	-0.0006(4)	-0.0029(9)	0.0021(16)
C(1)	0.1371(6)	0.1285(12)	0.0790(25)	0.0014(3)	0.0106(14)	0.0376(56)	0.0019(6)	0.0004(13)	0.0016(24)
CL(1)	0.1110(3)	0.6945(5)	0.0434(10)	0.0024(1)	0.0036(3)	0.0228(16)	-0.0003(2)	0.0002(4)	0.0019(7)
O(1)	0.0843(7)	0.7550(13)	0.0089(29)	0.0053(5)	0.0063(10)	0.0829(86)	0.0006(7)	-0.0106(20)	-0.0028(33)
O(2)	0.1062(11)	0.6616(13)	0.1774(30)	0.0103(10)	0.0106(15)	0.0469(68)	-0.0037(10)	-0.0152(21)	0.0107(27)
O(3)	0.1513(5)	0.7332(12)	0.0376(41)	0.0024(4)	0.0087(13)	0.1476(135)	0.0001(6)	0.0098(18)	0.0035(41)
O(4)	0.1040(10)	0.6380(12)	-0.0597(25)	0.0123(12)	0.0056(11)	0.0320(53)	0.0019(8)	-0.0068(20)	-0.0055(20)

ATOM	X/A	Y/B	Z/C	B(A**2)	ATOM	X/A	Y/B	Z/C	B(A**2)
C(216)	-0.010(1)	0.315(1)	0.115(3)	5.9(5)	C(111)	0.248(1)	0.254(1)	0.166(2)	4.1(4)
C(221)	0.057(1)	0.185(1)	0.365(2)	2.2(3)	C(112)	0.249(1)	0.288(1)	0.012(2)	3.2(4)
C(222)	0.090(1)	0.163(1)	0.470(3)	5.3(5)	C(113)	0.286(1)	0.290(1)	-0.086(2)	4.1(5)
C(223)	0.081(1)	0.094(1)	0.586(3)	7.5(6)	C(114)	0.325(1)	0.253(2)	-0.032(2)	4.9(4)
C(224)	0.045(1)	0.046(1)	0.559(3)	5.5(5)	C(115)	0.327(1)	0.228(1)	0.128(3)	7.9(7)
C(225)	0.011(1)	0.073(1)	0.459(3)	6.6(6)	C(116)	0.289(1)	0.219(1)	0.219(2)	4.5(5)
C(226)	0.017(1)	0.143(1)	0.357(3)	5.7(5)	C(121)	0.215(1)	0.356(1)	0.411(2)	2.5(4)
C(231)	0.056(1)	0.364(1)	0.365(2)	3.5(4)	C(122)	0.177(1)	0.409(1)	0.431(3)	5.5(5)
C(232)	0.036(1)	0.344(1)	0.513(2)	3.9(4)	C(123)	0.191(1)	0.484(1)	0.518(2)	4.5(5)
C(233)	0.027(1)	0.413(1)	0.615(3)	5.3(5)	C(124)	0.231(1)	0.497(1)	0.570(3)	7.2(7)
C(234)	0.044(1)	0.497(1)	0.579(3)	5.2(6)	C(125)	0.264(1)	0.447(1)	0.565(2)	4.5(4)
C(235)	0.062(1)	0.510(1)	0.433(2)	4.1(5)	C(126)	0.257(1)	0.372(1)	0.478(2)	4.5(5)
C(236)	0.072(1)	0.444(1)	0.326(2)	2.2(3)	C(131)	0.212(1)	0.179(1)	0.443(2)	2.5(4)
C(117)	0.210(1)	0.324(1)	-0.070(2)	2.1(4)	C(132)	0.211(1)	0.192(1)	0.595(2)	3.3(4)
C(118)	0.135(1)	0.353(1)	-0.148(2)	3.2(4)	C(133)	0.211(1)	0.124(1)	0.707(3)	6.8(6)
C(237)	0.095(1)	0.462(1)	0.180(2)	3.7(5)	C(134)	0.216(1)	0.044(1)	0.646(3)	5.2(5)
C(238)	0.118(1)	0.434(1)	-0.077(2)	2.6(4)	C(135)	0.217(1)	0.029(1)	0.480(2)	4.2(5)
N(3)	0.139(1)	0.059(1)	0.064(2)	2.4(4)	C(136)	0.214(1)	0.096(1)	0.377(3)	5.6(5)
C(2)	0.115(1)	-0.029(1)	0.069(3)	5.8(6)	C(211)	0.028(1)	0.266(1)	0.092(2)	4.2(5)
C(3)	0.153(1)	-0.067(2)	-0.039(4)	12.9(10)	C(212)	0.033(1)	0.220(1)	-0.048(2)	3.8(4)
C(4)	0.072(1)	-0.026(2)	0.015(4)	14.3(11)	C(213)	0.001(1)	0.213(1)	-0.153(2)	3.7(4)
C(5)	0.122(1)	-0.060(2)	0.226(4)	12.0(10)	C(214)	-0.039(1)	0.257(1)	-0.140(3)	5.9(5)
					C(215)	-0.045(1)	0.306(1)	-0.004(3)	7.7(7)

Table IV. Selected Physical and Spectroscopic Properties of New Compounds

	color	IR[a] ν_{CN}	IR[a] ν_{BF} or ν_{ClO}	^{1}H NMR[b] δ=CH	^{1}H NMR[b] δ_{CH_2}	^{1}H NMR[b] δ_{other}	^{31}P{^{1}H} NMR[c]
en=P_2 (1)	cream	1638		9.1 (d)[d]	4.67		
[Cu(en=P_2)]ClO_4 (2)	orange	1640	1100	8.54[e]	4.64		−4.16 (−80 °C)
[Ag(en=P_2)]BF_4 (3)	cream	1653	1080	8.65[f]	4.56		8.646 (J_{PAg} = 480, 560 Hz)
[Ni(en=P_2)]BF_4 (4)	yellow orange	1643	1060	9.16[f]	4.20		24.43 (in acetone)
[Cu(tn=P_2)]ClO_4 (5)	yellow	1638	1090	8.60[d]	3.43 (m)	1.65 (t)	−6.59 (−80 °C)
[Ni(tn=P_2)]$(BF_4)_2$ (6)	yellow	1630	1040	8.36 (d, br)[g]	4.40 (m)	2.50 (m)	
[Cu(en=P_2)(*t*-BuNC)]ClO_4 (7)	lemon yellow	2170, 1635, 1655	1090	8.60[f]	4.90	1.27	−3.35 (br, −80 °C)
[Ag(en=P_2)(*t*-BuNC)]BF_4 (8)	pale yellow	2187, 1650	1060	8.32[g]	4.77	1.30	7.38 (J_{PAg} = 462, 401)
[Ni(en=P_2)Br]Br (9)	chocolate	1628		9.19[h]	4.20		21.62 (−80 °C)

[a] IR spectra (cm^{-1}) were measured as mineral oil mulls. [b] All signals were singlets unless otherwise indicated: d, doublet; t, triplet; m, multiplet. Data for phenyl protons are not presented. [c] All ^{31}P NMR spectra were recorded in CH_2Cl_2, and chemical shifts downfield of the H_3PO_4 external standard are negative. [d] $CDCl_3$ solvent. [e] CD_3CN solvent. [f] $(CD_3)_2CO$ solvent. [g] CH_2Cl_2 solvent. [h] CD_2Cl_2 + Me_2SO-d_{10} solvent.

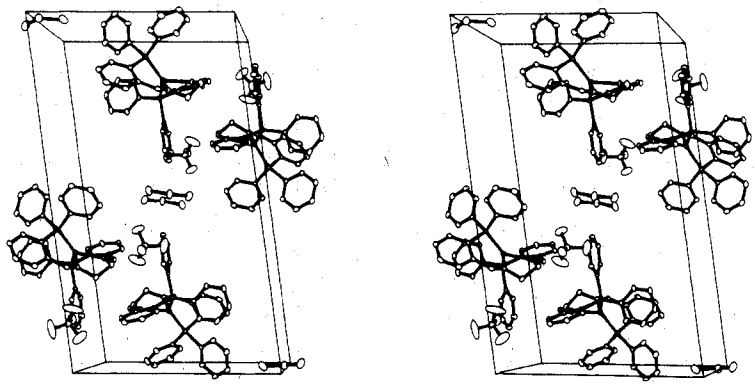

Figure 3. Stereoview of the crystal packing in [Cu(en=P_2)]ClO_4·CH_2Cl_2.

from alcohols. The structure of **1** clearly follows from its spectroscopic properties, notably the $\nu_{C=N}$ in the IR and its ^{1}H NMR spectrum (Table IV) which, like that of its aldehyde precursor, clearly shows the phosphorus coupling to the imino hydrogen. The related chelating agent derived from 1,3-diaminopropane (tn), abbreviated tn=P_2, was prepared similarly; however, it was not isolated.

Four-Coordinate Metal Complexes. Ligand **1** appears to react with most metal ions in solution; for the present study we have focused on the derivatives of nickel(II), copper(I), and silver(I) as these metals are capable of existing in a wide variety of coordination numbers and geometries, thus providing a range of templates for the binding of the new chelating agents. The related complexes of molybdenum(0), where the geometry is expected to be octahedral, will be described in a future publication. The reaction of equimolar quantities of the ligand with $[Cu(MeCN)_4]ClO_4$ and $AgBF_4$ affords the complexes [M(en=P_2)]X (M = Cu, X = ClO_4 (**2**); M = Ag, X = BF_4 (**3**)) as crystalline orange and pale yellow salts, respectively. Infrared spectra of these products show strong bands due to the imino group ($\nu_{C=N}$) and the counterions. For the tetrahedral geometry we can expect a singlet and an AA′BB′ multiplet for the methyne and methylene protons in the ^{1}H NMR spectrum, respectively. We observe, however, in addition to the singlet methyne and multiple phenyl signals, that the methylene resonance is a sharp singlet even down to −60 °C; furthermore **2** exhibits a broad ^{31}P{^{1}H} resonance at room temperature which sharpens only at −80 °C. The sharp methylene signal is likely due to a rapid interconversion between the enantiomeric forms of **2**. This rearrangement process could occur via a square-planar complex analogous to $[Ni(en=P_2)]^{2+}$ (vide infra) or via metal–ligand bond rupture followed by a twist and reassociation.

Ligand **1** reacts with nickel(II) fluoborate in acetonitrile to afford the yellow crystalline complex $[Ni(en=P_2)](BF_4)_2$ (**4**). IR and ^{1}H and ^{31}P{^{1}H} NMR results are similar to those found for **2** and **3** (see Table IV). The well-resolved ^{1}H NMR spectrum precludes appreciable paramagnetism and is consistent with at least an approximate square-planar geometry. This result is somewhat surprising since molecular models demonstrate that the bulky diphenylphosphino groups sterically clash in the square-planar geometry.

The ligand tn=P_2 reacts in a manner similar to en=P_2 with the appropriate copper and nickel salts to afford yellow products whose colors differed appreciably from $Cu(en=P_2)^+$ and $Ni(en=P_2)^{2+}$, apparently reflecting the impact of the expanded chelate backbone. This geometric freedom should be particularly important for the copper complex as it allows it to adopt the preferred tetrahedral geometry more easily. A more quantitative assessment of this change is provided by the electrochemical measurements (vide infra).

Structure of [Cu(en=P_2)]ClO_4. The structure consists of two independent Cu(I) cations, two perchlorate anions, and two molecules of dichloromethane, all separated by normal van der Waals distances. The cations have similar structures and are related by an approximate pseudocenter of symmetry at (0.23, 0.26, 0.52). There are small angular and conformational differences between the two chelate ring systems and a more pronounced difference in the orientation of the two phenyl rings which contain the atoms C(n11) and C(n21) (n = 1 for cation 1 and n = 2 for cation 2). The geometry and atom numbering for cation 1 are illustrated in Figure 1, and the crystal packing is shown by the stereopairs of Figure 3. Important bond lengths and angles are listed in Table V.

Table V. Principal Interatomic Distances (Å) and Angles (Deg) for $[Cu(en{=}P_2)]^+$

atoms	cation 1 (n = 1)	cation 2 (n = 2)
Cu(n)-P(n1)	2.227 (2)	2.221 (2)
Cu(n)-P(n2)	2.219 (2)	2.222 (2)
Cu(n)-N(n1)	2.083 (4)	2.049 (4)
Cu(n)-N(n2)	2.079 (4)	2.100 (4)
P(n1)-C(n11)	1.827 (5)	1.822 (5)
P(n1)-C(n21)	1.825 (5)	1.823 (5)
P(n1)-C(n31)	1.835 (5)	1.861 (5)
P(n2)-C(n41)	1.848 (5)	1.844 (5)
P(n2)-C(n51)	1.835 (5)	1.824 (5)
P(n2)-C(n61)	1.811 (5)	1.834 (5)
C(n31)-C(n32)	1.415 (7)	1.411 (7)
C(n32)-C(n1)	1.472 (9)	1.460 (8)
C(n1)-N(n1)	1.272 (7)	1.282 (7)
N(n1)-C(n2)	1.461 (8)	1.485 (7)
C(n2)-C(n3)	1.575 (8)	1.557 (8)
C(n3)-N(n2)	1.481 (7)	1.488 (6)
N(n2)-C(n4)	1.266 (7)	1.269 (7)
C(n4)-C(n42)	1.493 (7)	1.475 (7)
C(n42)-C(n41)	1.410 (7)	1.417 (6)
P(n1)-Cu(n)-P(n2)	133.04 (5)	128.63 (5)
N(n1)-Cu(n)-N(n2)	81.6 (2)	82.1 (2)
P(n1)-Cu(n)-N(n1)	89.2 (1)	92.7 (1)
P(n1)-Cu(n)-N(n2)	126.2 (1)	132.0 (1)
P(n2)-Cu(n)-N(n2)	92.2 (1)	89.6 (1)
Cu(n)-P(n1)-C(n11)	116.9 (2)	119.2 (2)
Cu(n)-P(n1)-C(n21)	124.1 (2)	120.6 (2)
Cu(n)-P(n1)-C(n31)	104.1 (2)	104.5 (2)
Cu(n)-P(n2)-C(n41)	105.6 (2)	105.4 (2)
Cu(n)-P(n2)-C(n51)	117.9 (2)	114.7 (2)
Cu(n)-P(n2)-C(n61)	121.0 (2)	123.0 (2)
C(n11)-P(n1)-C(n21)	104.3 (2)	105.4 (2)
C(n21)-P(n1)-C(n31)	103.6 (2)	103.6 (2)
C(n31)-P(n1)-C(n11)	100.5 (2)	100.6 (2)
C(n41)-P(n2)-C(n51)	102.2 (2)	103.1 (2)
C(n51)-P(n2)-C(n61)	102.9 (2)	103.4 (2)
C(n61)-P(n2)-C(n41)	105.1 (2)	105.2 (2)
P(n1)-C(n31)-C(n32)	120.8 (4)	120.8 (4)
P(n)-C(n31)-C(n36)	121.2 (4)	120.5 (4)
C(n32)-C(n31)-C(n36)	117.8 (5)	118.6 (5)
C(n31)-C(n32)-C(n1)	125.3 (5)	127.2 (5)
C(n31)-C(n32)-C(n33)	118.6 (5)	118.2 (5)
C(n33)-C(n32)-C(n1)	116.1 (5)	114.6 (5)
C(n32)-C(n1)-N(n1)	124.0 (5)	124.9 (5)
C(n1)-N(n1)-C(n2)	118.2 (4)	117.9 (4)
C(n1)-N(n1)-Cu(n)	130.4 (4)	129.4 (4)
C(n2)-N(n1)-Cu(n)	110.8 (3)	112.3 (3)
N(n1)-C(n2)-C(n3)	107.2 (5)	107.7 (4)
C(n2)-C(n3)-C(n2)	105.5 (4)	107.8 (4)
C(n3)-N(n2)-C(n4)	117.5 (5)	117.6 (4)
C(n3)-N(n2)-Cu(n)	110.7 (3)	110.5 (3)
C(n4)-N(n2)-Cu(n)	130.2 (3)	130.3 (3)
N(n2)-C(n4)-C(n42)	124.4 (5)	124.0 (5)
C(n4)-C(n42)-C(n41)	125.4 (5)	125.3 (4)
C(n4)-C(n42)-C(n43)	115.1 (4)	115.8 (4)
C(n41)-C(n42)-C(n43)	119.4 (4)	118.8 (4)
C(n42)-C(n41)-P(n2)	122.4 (3)	120.3 (3)
C(n46)-C(n41)-P(n2)	120.2 (4)	122.2 (4)
C(n42)-C(n41)-C(n46)	117.4 (4)	117.5 (4)

The ligand only permits a very distorted tetrahedral geometry at Cu and coordinates symmetrically such that the cation has an approximate (noncrystallographically imposed) C_2 axis along the bisector of the P–Cu–P angle (see Figure 1). The chelate "bite" angles, P(n1)–Cu(n)–N(n1), 89.2 (1) and 92.7 (1)°, P(n2)–Cu(n)–N(n2), 92.2 (1) and 89.6 (1)°, and N(n1)–Cu(n)–N(n2), 81.6 (2) and 82.1 (2)°, are not unusual for chelate rings of this type, but they are considerably smaller than ideal tetrahedral angles and result in correspondingly large P(n1)–Cu(n)–N(n2), 126.2 (1) and 132.0 (1)°, P(n2)–Cu(n)–N(n1), 126.0 (1) and 126.6 (1)°, and P(n1)–Cu(n)–P(n2), 133.04 (5) and 128.63 (5)°, angles. The average dihedral angle between the planes P(n1)–Cu(n)–P(n2) and N(n1)–Cu(n)–N(n2) is 120°. The ideal value for undistorted tetrahedral geometry is 90°, and this difference further emphasizes the constraints of the chelating ligand. Qualitatively similar, although less extreme, distorted tetrahedral geometries have been observed in Cu(I) complexes of the type $[Cu(L{-}L)(PPh_3)_2]$ (L–L is a bidentate anion), and it has been suggested that the smaller "bite" angles (range 57.5–103.0°) and lower steric bulk of the anionic ligands are repsonsible for the correspondingly larger P–Cu–P angles (range 133.4–120.0°).[22] The Cu–P distances in both cations range from 2.219 (2) to 2.227 (2) Å, and the average value of 2.222 Å is somewhat shorter than the range of values (2.24–2.29 Å) typically observed for pseudotetrahedral Cu(I) complexes having two monodentate phosphorus ligands.[23,24] Cu(I)–P distances are apparently rather insensitive to the exact geometry at the metal, but it has been suggested that they are sensitive to steric crowding.[23] The short Cu–P distances observed here may therefore reflect a reduction in the importance of ligand–ligand nonbonding interactions for a complex containing a chelating ligand.

The Cu–N distances in cation **1**, 2.083 (4) and 2.079 (4) Å, are not significantly different and average 2.081 Å. In contrast, the Cu–N distances in cation **2**, 2.049 (4) and 2.100 (4) Å, differ by 0.051 Å, but their average value of 2.08 Å is identical with that in cation 1. These values may be compared with the slightly longer Cu(I)–imine distances of 2.100 (2)–2.165 (2) Å, found for a square-pyramidal Cu(I) complex with a basal macrocyclic tetraimine ligand and an apical CO group.[25]

The C=N, C–N, and C–C distances within the chelate rings are comparable with the values which have been found in copper(II) *o*-hydroxyacetophenone imine[26] and salicylaldimine[27] complexes. The nitrogen atoms have trigonal-planar geometries with a small pyramidal distortion. There are marked distortions from the ideal sp^2 angles of 120°, the Cu–N–C angles in the five- and six-membered rings having angles of ca. 111 and 130°, respectively. Similarly, the Cu–P–C angles in the six-membered rings have values of ca. 105°, which is smaller than the value of ca. 114° normally observed for M–P substituent angles in nonchelating phosphorus ligands. The remaining angles within the phenyl and phenylene rings are normal, and the rings show little significant deviation from planarity.

The perchlorate anions each have one well-resolved oxygen atom; the others are less well defined and have substantially higher and more anisotropic temperature factors. This suggests that there is either some rotational disorder or oscillation about the O(11)–Cl(1) and O(24)–Cl(2) axes in these anions and the derived bond distances and angles are affected accordingly.

Reactions of Four-Coordinated Complexes. The complexes **2–4** all react readily with additional ligands to form isolable adducts. Addition of *tert*-butyl isocyanide (*t*-BuNC) to solutions of **2** and **3** results in formation of the complexes $[M(en{=}P_2)(t\text{-BuNC})]X$ (M = Cu, X = ClO_4 (**7**); M = Ag, X = BF_4 (**8**)) isolated as golden and pale yellow crystals, respectively. The infrared spectrum of compound **7** is very similar to that of complex **2**, except for an additional band for the isocyanide $\nu_{C\equiv N}$ and the split imine absorption which is

(22) Drew, M. G. B.; Biothma, A. H.; Edwards, D. A.; Richards, R. *Acta Crystallogr., Sect. B* **1975**, *B31*, 2695–2697 and references therein.
(23) Gill, J. T.; Mayerle, J. J.; Welcker, P. S.; Lewis, D. F.; Ucko, D. A.; Barton, D. J.; Stowens, D.; Lippard, S. J. *Inorg. Chem.* **1976**, *15*, 1155–1168.
(24) Camus, A.; Marsich, N.; Nardin, G.; Randaccio, L. *J. Chem. Soc., Dalton Trans.* **1975**, 2560–2565.
(25) Gagné, R. R.; Allison, J. L.; Gall, R. S.; Koval, C. A. *J. Am. Chem. Soc.* **1977**, *99*, 7170–7178.
(26) Kirchner, R. M.; Andreetli, G. D.; Barnhart, D.; Thomas, F. D.; Welsh, D.; Lingafelter, E. C. *Inorg. Chim. Acta* **1973**, *7*, 17–42.
(27) Lingafelter, E. C.; Braun, R. L. *J. Am. Chem. Soc.* **1966**, *88*, 2951–2956.

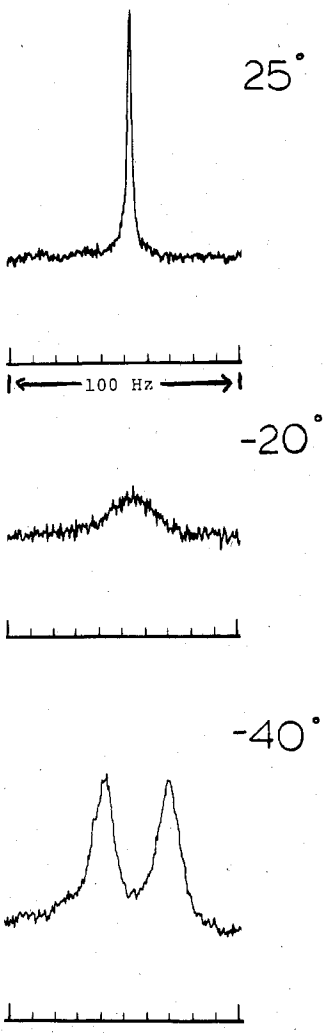

Figure 4. 220-MHz ^1H NMR spectra of $[Cu(en{=}P_2)(t\text{-BuNC})]ClO_4$ (CD_2Cl_2 solution) at various temperatures.

observed both as a Nujol mull and in CH_2Cl_2 solution, indicating two imine environments; for the silver complex, **8**, $\nu_{C=N}$ occurs as a single absorbance both as a mull and in CH_2Cl_2 solution. The crystal structure of **7** (vide infra) reveals that the *t*-BuNC has displaced one of the imine donors of the en=P_2 ligands. At variance with these observations, the ^1H NMR spectrum of **7** is very simple, suggestive of the lability expected for a d^{10} complex. The ambient-temperature ^1H NMR of **7** resembles that for **2** with an additional singlet for the *tert*-butyl group; however, as shown in Figure 4 cooling to −40 °C causes the methylene singlet to split into a broad doublet attributable to an unresolved AA'BB' system indicative of an exchange rate of ca. 70 s^{-1} at −20 °C. The ^1H NMR spectrum (35 °C) of a mixture of **2** and **7** shows no splitting of the methylene or methyne singlets; nor is splitting of the *tert*-butyl resonance observed in solutions of **7** and excess *t*-BuNC.

The ambient-temperature $^{31}P\{^1H\}$ NMR spectrum of **7** consists of a broad singlet which sharpens somewhat on cooling to −80 °C (width at half-height is 100 Hz). The observation of asymmetric, albeit broad singlet in the low-temperature ^{31}P NMR spectrum and the sharp singlet for the imino protons at −40 °C supports the argument that a low-energy intramolecular site exchange occurs as shown in Figure 5. The residual broadness in the −80 °C ^{31}P NMR spectrum is related to the remaining exchange which at 40 °C is occurring at a rate fast on the ^1H NMR time scale. That the observation of only one imino proton is *not* due to an accidental degeneracy

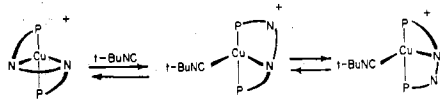

Figure 5. Proposed scheme for the reaction of $[Cu(en{=}P_2)]^+$ with *t*-BuNC and associated dynamic behavior.

is supported by the fact that, in the complex $Mo(en{=}P_2)(CO)_3$ wherein en=P_2 is bound in an unsymmetrical P–N–N manner, the two nonequivalent imine protons are easily resolved. The detailed mechanism by which **7** undergoes imine site exchange could involve either a three-coordinate[28] PPC bound intermediate or a five-coordinate PNNPC intermediate (eq 1).

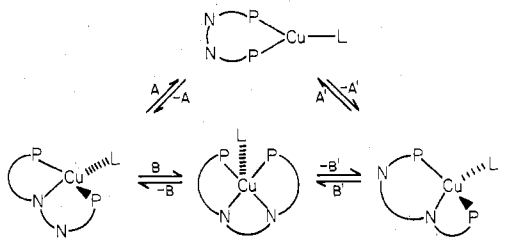

(1)

While there exists good precedent for both coordination numbers in the chemistry of copper(I), we favor the intermediacy of a PNNPC complex because of its similarity to the five-coordinate complexes $[Ag(en{=}P_2)(t\text{-BuNC})]^+$ and $[NiBr(en{=}P_2)]^+$.

Scheme I also applies to the analogous tn=P_2 complex where we find that addition of stoichiometric quantities of *t*-BuNC to $CHCl_3$ solutions of $[Cu(tn{=}P_2)]ClO_4$ ($\nu_{C=N}$ = 1638 cm^{-1}) results in the splitting of the imine absorption ($\nu_{C=N}$ = 1692 and 1640 cm^{-1}) with concomitant appearance of the isocyanide band. On a preparative scale this reaction results in a color change to lemon yellow as found for the conversion of **2** and **7**; addition of diethyl ether however resulted in the precipitation of pure $[Cu(tn{=}P_2)]ClO_4$. Nonetheless these solution results clearly indicate that the $Cu(tn{=}P_2)^+$ also undergoes a displacement of an internal imine donor forming in this case a *ten-membered chelate ring*. The fact that the binding of the isocyanide in $[Cu(tn{=}P_2)(t\text{-BuNC})]ClO_4$ is weaker than that in **7** is consistent with the idea that the driving force for adduct formation derives at least in part from the release of strain energy inherent in the distorted tetrahedral complex **2**.[29] Apparently, by virtue of the extra methylene group, tn=P_2 more comfortably binds to the copper ion, and less strain energy is released in going to $[Cu(tn{=}P_2)(t\text{-BuNC})]^+$.

The ^{31}P NMR spectrum of the silver complex **8** consists of well-resolved doublet of doublets at room temperature arising from $J_{P^{109}Ag}$ and $J_{P^{107}Ag}$. As the solution IR spectrum of **8** shows only one $\nu_{C=N'}$ the complex is either a three-coordinate complex containing the PCP donor set and a 13-membered chelate ring which we feel is unlikely or a five-coordinate complex. The 220-MHz ^1H NMR spectrum of **8** remains unchanged upon cooling to −50 °C indicative that this complex is more labile than the analogous copper compound consistent with the fact that rates of ligand rearrangements of metal complexes of d^{10} configuration increase with increasing ionic radius.[30]

Reaction of nickel(II) bromide with **1** affords a brown complex which we formulate as $[NiBr(en{=}P_2)]Br$ (**9**). The

(28) Eller, P. G.; Bradley, D. C.; Hursthouse, M. B.; Meek, D. W. *Coord. Chem. Rev.* **1977**, *24*, 1–95.

(29) An attempt to obtain accurate equilibrium binding constants for the reaction of **2** (5×10^{-4} M) with *t*-BuNC (5×10^{-4} to 10^{-2} M) revealed nonisobestic behavior and only small spectral changes.

(30) Holm, R. H. In "Dynamic Nuclear Magnetic Resonance Spectroscopy"; Jackman, L. M., Cotton, F. A., Eds.; Academic Press, New York, 1975; pp 317–376.

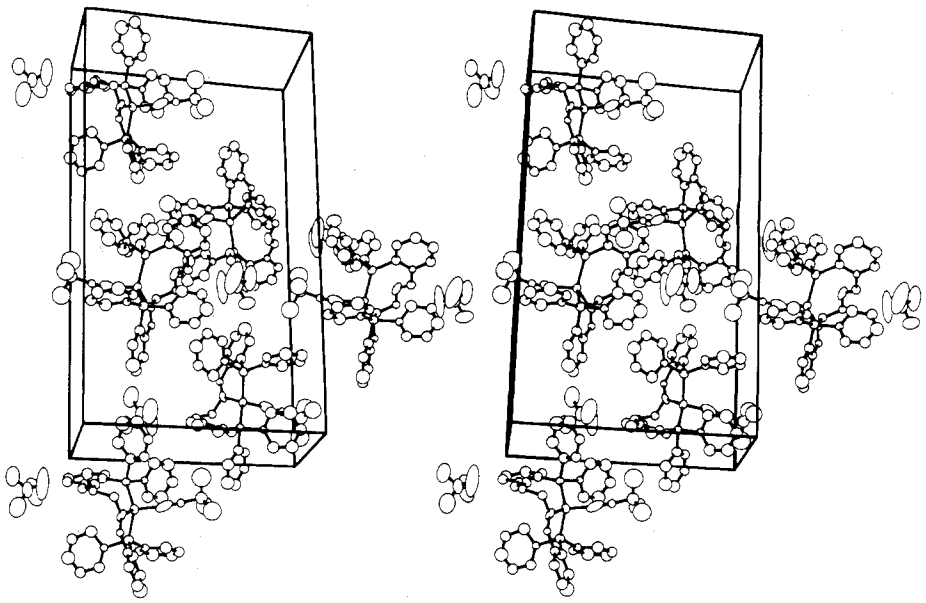

Figure 6. Stereoview of the crystal packing in $[Cu(en{=}P_2)(t\text{-BuNC})]ClO_4$.

electronic absorption spectrum of **9** (615 (sh), 475 nm (sh); ϵ 1700) is similar to that reported for [NiBr(PNNP)]Br (650 (sh), 495 nm; ϵ 390)[31] where PNNP is the diaminodiphosphine

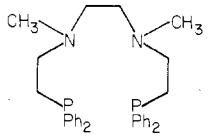

PNNP

The coordination of one bromide is confirmed by the observation that the electronic absorption spectrum of **9** remains unchanged upon dilution with less than 1 equiv of **4**; this result is explained by eq 2. As in the case of most other complexes

$$[NiBr(en{=}P_2)]^+Br^- + [Ni(en{=}P_2)]^{2+} \rightarrow 2[NiBr(en{=}P_2)]^+ \quad (2)$$

described in this paper, the ^1H NMR spectrum for **9** is very simple, even at −50 °C (Table IV). The absorptions due to the methylene and methyne resonances are shifted to lower field than those found for complexes **2**–**6**, demonstrating that the coordinated bromide ligand has substantial influence on the local magnetic field about the ligand. Titration of $[NiBr(en{=}P_2)]Br$ with excess **4** causes the methyne and methylene peaks to shift toward the resonant positions found for pure **4**, consistent with facile halide exchange between **4** and the cation $[NiBr(en{=}P_2)]^+$ (eq 3).

$$[Ni^*Br(en{=}P_2)]^+ + [Ni(en{=}P_2)]^{2+} \rightleftarrows [Ni^*(en{=}P_2)]^{2+} + [NiBr(en{=}P_2)]^+ \quad (3)$$

Structure of $[Cu(en{=}P_2)(t\text{-BuNC})]ClO_4$. The crystal is comprised of distinct ionic units separated by normal van der Waals contacts. The geometry and atom numbering of the cation are shown in Figure 2, and the crystal packing is illustrated by the stereo pairs in Figure 6. Important bond lengths and angles in the cation are listed in Table VI.

In $[Cu(en{=}P_2)(t\text{-BuNC})]^+$ the isocyanide has replaced one of the imine nitrogens coordinated to copper in $[Cu(en{=}P_2)]^+$. A structural consequence is the relief of some of the angular strain evident (vide supra) in the latter cation. Only the P(1)–Cu–N(1) "bite" angle is now constrained to be small, and distortion from tetrahedral geometry at copper is consequently less severe. The Cu–P distances in $[Cu(en{=}P_2)(t\text{-BuNC})]^+$ (2.255 and 2.301 Å) are longer than in $[Cu(en{=}P_2)]^+$ (mean 2.222 Å), and as previously suggested this may reflect greater steric crowding in the former cation.

The internal angles of that part of the chelate ring P(1) through N(1) follow the trend for the cation $[Cu(en{=}P_2)]^+$ described above. The other half of the chelate ring is less

Table VI. Bond Lengths (Å) and Angles (Deg) for the Cation $[Cu(en{=}P_2)(t\text{-BuNC})]^+$[a]

Cu-P(1)	2.255 (5)	P(1)-Cu-P(2)	123.7 (2)
Cu-P(2)	2.301 (5)	P(1)-Cu-N(1)	92.1 (4)
Cu-N(1)	2.05 (1)	P(1)-Cu-C(1)	107.8 (6)
Cu-C(1)	2.01 (2)	P(2)-Cu-N(1)	121.1 (4)
		P(2)-Cu-C(1)	102.5 (6)
		N(1)-Cu-C(1)	108.8 (7)
N(3)-C(1)	1.15 (2)	C(112)-C(117)-N(1)	127 (2)
N(3)-C(2)	1.49 (2)	C(236)-C(237)-N(2)	123 (2)
C(2)-C(3)	1.55 (3)	C(117)-N(1)-C(118)	115 (1)
C(2)-C(4)	1.40 (3)	C(117)-N(1)-Cu	129 (1)
C(2)-C(5)	1.43 (3)	C(118)-N(1)-Cu	115 (1)
		N(1)-C(118)-C(238)	108 (1)
		C(118)-C(238)-N(2)	109 (1)
		C(238)-N(2)-C(237)	120 (1)
P(1)-C(111)	1.76 (2)	Cu-C(1)-N(3)	167 (2)
P(1)-C(121)	1.87 (2)	C(1)-N(3)-C(2)	170 (2)
P(1)-C(131)	1.84 (2)	N(3)-C(2)-C(3)	97 (2)
P(2)-C(211)	1.82 (2)	N(3)-C(2)-C(4)	103 (2)
P(2)-C(221)	1.84 (2)	N(3)-C(2)-C(5)	108 (2)
P(2)-C(231)	1.87 (2)		
C(112)-C(117)	1.50 (2)	C(113)-C(112)-C(117)	111 (2)
C(117)-N(1)	1.30 (2)	C(111)-C(112)-C(117)	124 (2)
N(1)-C(118)	1.54 (2)	C(231)-C(236)-C(237)	123 (2)
C(118)-C(238)	1.54 (2)	C(235)-C(236)-C(237)	120 (1)
C(238)-N(2)	1.42 (2)		
N(2)-C(237)	1.27 (2)		
C(237)-C(236)	1.45 (2)		
Cu-P(1)-C(111)	106.2 (6)	P(1)-C(111)-C(112)	125 (1)
Cu-P(1)-C(121)	122.0 (6)	P(2)-C(231)-C(236)	120 (1)
Cu-P(1)-C(131)	115.4 (6)		
Cu-P(2)-C(211)	115.2 (7)		
Cu-P(2)-C(221)	105.2 (5)		
Cu-P(2)-C(231)	124.9 (6)		

[a] Bond lengths and angles in the phenyl groups and the perchlorate anion are contained in the supplementary material.

(31) Sacconi, L.; Dei, A. *J. Coord. Chem.* **1979**, *1*, 229–236. This paper refers to an unpublished structure of $[Ni(PNNP)]Br_2{\cdot}0.5C_2H_5OH$ by C. Mealli and L. Sacconi in 1971.

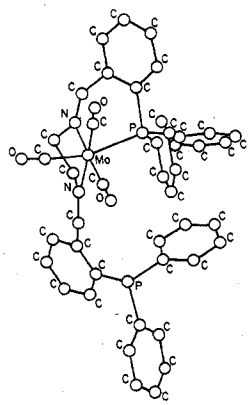

Figure 7. ORTEP drawing of $Mo(en{=}P_2)(CO)_3$ with thermal ellipsoids at the 50% probability level.[32]

Table VII. Reduction Potentials (V) for New Complexes Derived from Dc Cyclic Voltammetry Relative to Ag/AgCl[a]

$Ni(en{=}P_2)^{2+}$	$\xrightarrow{-0.302}$	$Ni(en{=}P_2)^{+}$	$\xrightarrow{-0.837}$	$Ni(en{=}P_2)^{0}$
$Ni(tn{=}P_2)^{2+}$	$\xrightarrow{-0.22}$	$Ni(tn{=}P_2)^{+}$	$\xrightarrow{-0.84}$	$Ni(en{=}P_2)^{0}$
$Cu(en{=}P_2)^{3+}$	$\xrightarrow{[+1.37]}$	$Cu(en{=}P_2)^{2+}$	$\xrightarrow{0.77}$	$Cu(en{=}P_2)^{+}$
		$Cu(tn{=}P_2)^{2+}$	$\xrightarrow{[0.85]}$	$Cu(tn{=}P_2)^{+}$
		$Ag(en{=}P_2)^{2+}$	$\xrightarrow{[1.17]}$	$Ag(en{=}P_2)^{+}$

[a] Values shown in brackets are only partially reversible couples.

strained. Although the Cu–P(2)–C(231) angle is somewhat larger (124.9°) than usual, the P(2)–C(231)–C(236), C(231)–C(236)–C(237), C(236)–C(237)–N(2), and C(237)–N(2)–C(238) angles do not differ significantly from their expected value (120°). The geometry of the *tert*-butyl isocyanide ligand is unexceptional, the Cu–C–N–C skeleton being very roughly linear. The complex is a unique example of a *9-membered chelate ring* bound to a tetrahedrally coordinated metal. This unusual 6–9 P–N–P tridentate chelate is likely to be a result of geometric considerations rather than a preference of Cu(I) for phosphine over imine donors. A tetrahedral geometry at a transition-metal atom can more comfortably accommodate 6–9 rings than 6–5 rings because of the preference for a large "bite" angle at the metal. In an octahedral complex, with a smaller prefered "bite" angle, a 6–5 ring might be anticipated. It is interesting to note that the exchange-inert $Mo(CO)_3(en{=}P_2)$ also contains the chelate bound in a tridentate manner (Figure 7). However this complex has been shown by X-ray crystallography to be more usual 6–5 P–N–N linkage isomer.[32]

Electrochemistry. The rich redox chemistry characteristic of the chelating phosphine, arsine, and imine ligands was sought in the title complexes, and as shown in Table VII the shuttling of these complexes between the d^8, d^9, and d^{10} configurations occurs with varying degrees of reversibility.

The stepwise reduction of square-planar Ni(II) complexes has been observed previously,[33] although as yet few attempts have been made toward the characterization of Ni(I) derivatives spectroscopically much less structurally.[34] The ac and dc cyclic voltamogram for $[Ni(en{=}P_2)]^{2+}$ is illustrated in Figure 8 as well as the results of the spectrophotometric monitoring of the first reduction using constant-potential electrolysis (Figure 9). Experiments with $[Cu(en{=}P_2)]ClO_4$

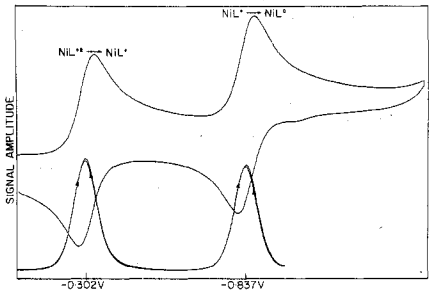

Figure 8. Ac and dc cyclic voltammograms for the reduction of $[Ni(en{=}P_2)](BF_4)_2$ in 0.1 M Et_4NClO_4 in acetone relative to Ag/AgCl (scan rate = 100 mV/s).

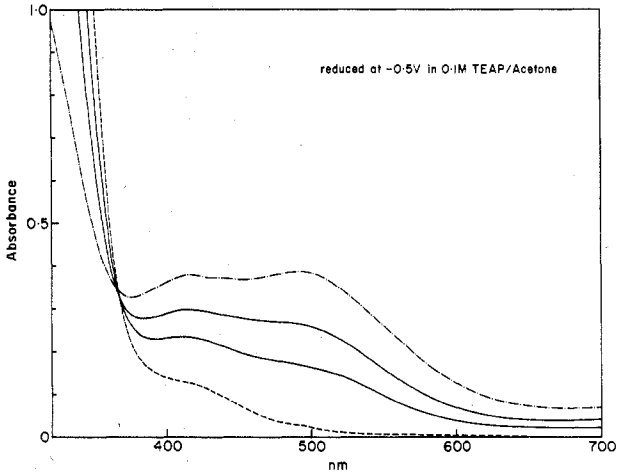

Figure 9. Spectrophotometric monitor of the one-electron reduction of $[Ni(en{=}P_2)](BF_4)_2$ (---).

demonstrate the accessibility of the Cu(II) and Cu(III) derivatives although the latter couple is only partially reversible under our conditions (200 mV/s sweep). Addition of *t*-BuNC completely quenches all redox chemistry for the Cu(I) and Ag(I) complexes of $en{=}P_2$, consistent with the tendency of the isocyanide to stabilize the lower oxidation state.

The comparison of the en and tn derived ligands is illustrative of the influence of the chelate bite angle on the redox potentials. Whereas it is clear than $en{=}P_2$ effectively stabilizes Cu(I) relative to Cu(II), this stabilization likely suffers from the inability of this ligand to comfortably accommodate the geometric preference of the cuprous ion. Consistent with this, expansion of the N···N bite angle in going from $en{=}P_2$ to $tn{=}P_2$ results in the increased Cu(II)/Cu(I) reduction potential reflecting the greater ability of $tn{=}P_2$ to adopt the tetrahedral geometry. This effect has been noted previously where values of $\Delta E_{1/2}$ ($=E_{1/2}(tn) - E_{1/2}(en)$) ranged from 0.18 to 0.30.[35] A smaller effect is found for the Ni(II)/Ni(I) couple where $\Delta E_{1/2} = 0.08$; here one expects that, since the geometries of both Ni(II) and Ni(I) are likely square planar, the effect should be small. It is somewhat surprising at first that the Ni(I)/Ni(0) couple is not more sensitive to the expansion of the chelate backbone; this presupposes, however, that the zerovalent nickel binds to the chelating agent in a conventional manner. Alternative binding modes include the η^2-bonded imine(s) or dissociation of one N donor to afford a 16e NiL_3 complex.

Summary. The tetradentate iminophosphines have been shown to function as chelating agents of unusual geometric and electronic adaptability. Spectroscopic and crystallographic evidence suggests that the ligands are capable of adopting the

(32) Jeffery, J. C.; Rauchfuss, T. B.; Tucker, P. A., unpublished results.
(33) Martelli, M.; Pilloni, G.; Zotti, G.; Daolio, S. *Inorg. Chim. Acta* **1974**, *11*, 155–158.
(34) Sacconi, L.; Ghilardi, C. A.; Mealli, C.; Zambini, F. *Inorg. Chem.* **1975**, *14*, 1380–1386.
(35) Patterson, G. S.; Holm, R. H. *Bioinorg. Chem.* **1975**, *4*, 257–275.